Electron Counting Spectroscopy of CdSe Quantum Dots

Mariusz Zdrojek, Maria Jose Esplandiu, Amelia Barreiro, and Adrian Bachtold*

CIN2(CSIC-ICN), Campus UAB, E-08193 Bellaterra, Spain

(Received 2 December 2008; published 5 June 2009)

We report on the electronic properties of semiconducting CdSe quantum dots that can be filled or emptied with many electrons. To accomplish that, we employ a device layout where the investigated quantum dot is attached to only one electrode, a carbon nanotube. Measurements consist of detecting individual electrons transferred onto the quantum dot (by monitoring the nanotube resistance) while sweeping the electrochemical potential of the dot with a gate. This technique allows us to detect the energy gap of the semiconducting quantum dot and to access many electronic levels. We exploit the latter finding to study the statistical aspects of the spectrum of the quantum dot. The measured spectrum distribution approaches the bimodal Wigner distribution, which is the most basic prediction of the random matrix theory applied to quantum dots.

DOI: 10.1103/PhysRevLett.102.226804 PACS numbers: 73.22.Dj, 73.23.Hk, 73.63.Kv

Semiconducting quantum dots synthesized via colloidal chemistry techniques have generated considerable interest in the science and technology at the nanoscale [1]. One reason is that quantum dots can be described as ''artificial atoms'' for which the electronic spectrum is controlled by the size of the dot. This is due to quantum confinement where the wave function has to satisfy the boundary conditions of the dot. The properties of quantum dots can be further tailored by adding charge carriers to obtain ''ionized artificial atoms.'' This can be achieved via doping with intentional impurities or by electrostatic means where a voltage is applied to a gate electrode [2]. This excess charge has been employed to tune the optical and electrical properties [3–9]. However, the amount of excess charge carriers obtained with current methods remains modest (between 1 and 10).

In this Letter, we study the electronic properties of semiconducting CdSe quantum dots using a new device layout. It allows us to fill or empty the dots with many electrons (possibly as many as 200). Measurements are carried out using a new technique that detects individual electrons transferred onto the quantum dot. This technique, which we call electron counting spectroscopy, enables the study of the spectrum of the electronic levels. In particular, we observe the energy gap of the semiconducting quantum dot. Since many electronic levels can be accessed, we also investigate the statistical aspects of the spectrum. The spectrum distribution is composed of a peak and a broad tail, which are attributed to the charging energy and the (fluctuating) level spacing, respectively. This result is consistent with the bimodal Wigner distribution, a prediction of the random matrix theory for quantum dots that has not been experimentally demonstrated until now.

Our devices have a new layout. The CdSe quantum dots are electrically probed using single-wall carbon nanotubes as contact electrodes. In previous experiments, colloidal quantum dots could not be filled or emptied with many electrons. The reason lies in the small size of the dots compared to the large source and drain metal electrodes that were employed. Indeed, these electrodes screen the electric field between the gate and the dot very effectively (the gate voltage is used to change the number of electrons N in the dot) [Fig. 1(a)]. A way to decrease the screening is to attach electrodes of the same size as the quantum dot [Fig. 1(b)]. For this, we employ metallic single-wall carbon nanotubes. Another new feature in the device layout is that a single electrode (a nanotube) contacts the CdSe quantum dot [Fig. 2(a)]. This greatly simplifies the fabrication process compared to standard devices with two electrodes (source and drain), which have to be separated by a few nanometers gap.

Devices were fabricated by means of standard nanofabrication techniques. Carbon nanotubes were grown by means of chemical vapor deposition on a doped Si wafer with a 1 μm thermal silicon oxide layer. They were electrically contacted to Cr/Au electrodes patterned by electron-beam lithography. CdSe quantum dots ($\sim$5 nm diameter) were deposited onto the wafer from a colloid suspension and were found to be preferentially adsorbed onto nanotubes [10]. Figure 2(b) shows an atomic force microscopy image of a device. We notice that there are about three quantum dots lying on the nanotube, although we will demonstrate later on that only one of them is probed.

The electron properties of the CdSe quantum dot are detected by means of the electron counting spectroscopy

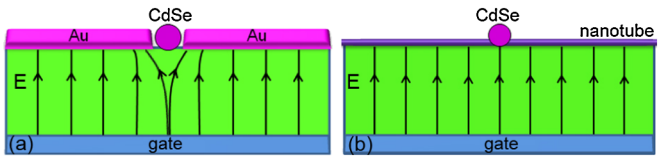

FIG. 1 (color online). Screening of the electric field by the electrodes. (a) A quantum dot attached to large source and drain metal electrodes. (b) A quantum dot attached to a nanotube electrode.

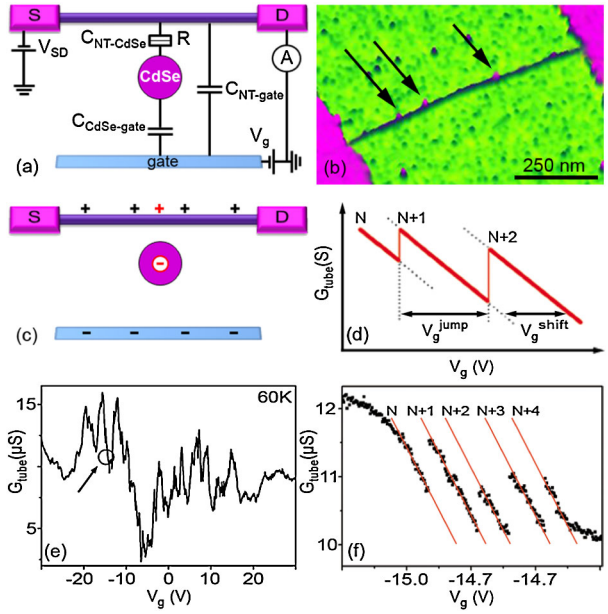

FIG. 2 (color online). Electron counting spectroscopy. (a) Equivalent electrical circuit of a quantum dot attached to a nanotube electrode. Individual electrons tunnel between the quantum dot and the nanotube through the tunnel resistance R. (b) Atomic force microscopy image of a device with a 1 μm long carbon nanotube decorated with about three CdSe quantum dots (labeled by arrows). We show in the text that only the electron properties of a single quantum dot are probed. (c) Schematic illustrating the transfer of an electron onto the dot. (d) Schematic of a $G_{\text{tube}}(V_g)$ curve. (e) G_{tube} as a function of V_g. The irregular oscillations are due to disorder in the nanotube [36]. (f) $G_{\text{tube}}(V_g)$ over a narrow V_g scan. Each shift of $G_{\text{tube}}(V_g)$ is attributed to a single electron transfer.

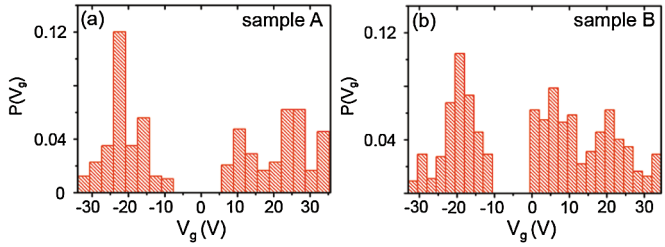

FIG. 3 (color online). Energy gap of semiconducting CdSe quantum dots. (a) Histogram of the number of electrons transferred onto the dot for sample A. The average number of shifts from the gap to $V_g = -35V(+35V)$ is 181(192). (b) Histogram for sample B. The width of the V_g gap is similar to the one in (a), but the gap is shifted towards lower V_g values. This is attributed to uncontrolled doping generated during nanofabrication. The average number of shifts from the gap to $V_g = -35V(+35V)$ is 168(235).

technique. It consists of measuring the conductance of the nanotube G_{tube} as a function of the voltage applied on the gate V_g [Figs. 2(a) and 2(e)]. Sweeping V_g allows us to change N. Measuring G_{tube} allows the detection of the transfer of individual electrons between the quantum dot and the nanotube [11].

The effect of an extra electron on the quantum dot is to shift the $G_{\text{tube}}(V_g)$ curve along the V_g axis [Fig. 2(d)]. This can be understood using the electric circuit shown in Fig. 2(a), which consists of a network of 3 capacitances. When an extra electron tunnels into the quantum dot, the nanotube must accommodate the opposite charge due to the tube-dot capacitance [Fig. 2(c)]. In a first approximation, this causes the same effect on G_{tube} as does changing V_g (G_{tube} is proportional to the charge density of the nanotube, which depends on V_g through the tube-gate capacitance).

Figure 2(f) shows measurements of $G_{\text{tube}}(V_g)$ shifts. We have shown in Ref. [11] that every shift corresponds to the transfer of a single electron. We emphasize that our method to count electrons allows us to tell whether electrons tunnel into or out of the dot. Electrons tunneling into the dot (obtained by increasing V_g) causes the $G_{\text{tube}}(V_g)$ curve to shift to the right along the V_g axis [Fig. 2(f)]. Otherwise, the shift occurs to the left. The direction of the tunnel process is remarkably well controlled. Ninety-eight percent of the shifts occur to the right when V_g is increased [12].

Figures 3(a) and 3(b) show the number of shifts in $G_{\text{tube}}(V_g)$ measured as a function of V_g over a large range of voltages, from -35 to $+35$ V. Shifts are observed everywhere except in the region around $V_g = 0$ V. This V_g gap is attributed to the energy gap of the semiconducting CdSe quantum dot. Indeed, no electron can tunnel into the dot, as there are no free states available. Note that we only consider the shifts in which the $G_{\text{tube}}(V_g)$ curves remain parallel before and after the shift such as in Fig. 2(f)]. This excludes a small fraction of shifts ($\sim$10%). Such handling of the data is justified in that such shifts are observed in devices on which CdSe quantum dots have not been deposited. We attribute these to charges trapped inside, for instance, the silicon oxide.

The number of shifts is about 200 when sweeping V_g from the energy gap to either -35 V or $+35$ V. This suggests that the quantum dot can be filled or emptied with as many as 200 electrons, assuming that a single quantum dot is probed (see below). This number corresponds to about $0.08e$ for each atom of the dot. This is much more than previous transport or optical experiments on semiconducting quantum dots [3–9]. This concentration of electrons in a small volume generates a high electric field. We get a field $\xi \simeq 20$ V/nm at the surface of the dot using $\xi = 200e/(4\pi\epsilon_0\epsilon_r r^2)$ with $r = 2.5$ nm and $\epsilon_r \simeq 2$ the average dielectric constant of the environment. Such a field is extreme but is comparable to the one of fullerenes charged with a few electrons [13]. We notice, however, that we cannot exclude that some of the electrons may be lost by emission into the nearby environment [14].

We now turn our attention to the spectrum of CdSe quantum dots by looking at V_g^{shift} [the amount that $G_{\text{tube}}(V_g)$ shifts along the V_g axis]. V_g^{shift} is proportional to the energy required to add one electron,

$$V_g^{\text{shift}} = \alpha E_{\text{ad}}, \tag{1}$$

where α depends on the capacitances between the quantum dot, the nanotube, and the gate [12]. When the signal of G_{tube} is particularly clean, we find that V_g^{shift} can oscillate for successive N [Fig. 4(a)], consistent with the spin-related even-odd effect (see below). When plotting the distribution of V_g^{shift}, we obtain a peak at about 100 mV and a long tail at higher energies [Figs. 4(c) and 4(d)].

We here discuss the possible origins of the distribution of V_g^{shift}. It may be related to the density of states of CdSe. This is however not the case, since the fluctuation remains similar when varying V_g [Fig. 4(e)]. Another possibility is that the distribution is affected by the emission of electrons from the dot into the environment. This may smear the distribution and give it a Gaussian shape. It is unlikely that it results in the measured peak flanked by a tail. An alternative explanation may be that there are several quantum dots lying on the nanotube. However, we have fabricated 20 similar devices, and only two of them exhibit shifts with parallel $G_{\text{tube}}(V_g)$ curves [Fig. 2(f)]. The vast majority of dots are thus inactive. In the unlikely case that one of the two devices should probe two dots, the number of shifts would be twice as many and the average separation $\langle V_g^{\text{jump}} \rangle$ between the shifts [Fig. 2(d)] would be half as much. However, $\langle V_g^{\text{jump}} \rangle$ for samples A and B is 156 mV and 146 mV, respectively. Overall, it is likely that one single quantum dot is probed. This is probably because the nanotube-dot resistance has to lie within the appropriate range. If it is too large, shifts will never occur. In the opposite case, tunneling events will be so fast that electrons will tunnel in and out repeatedly, smearing the shifts.

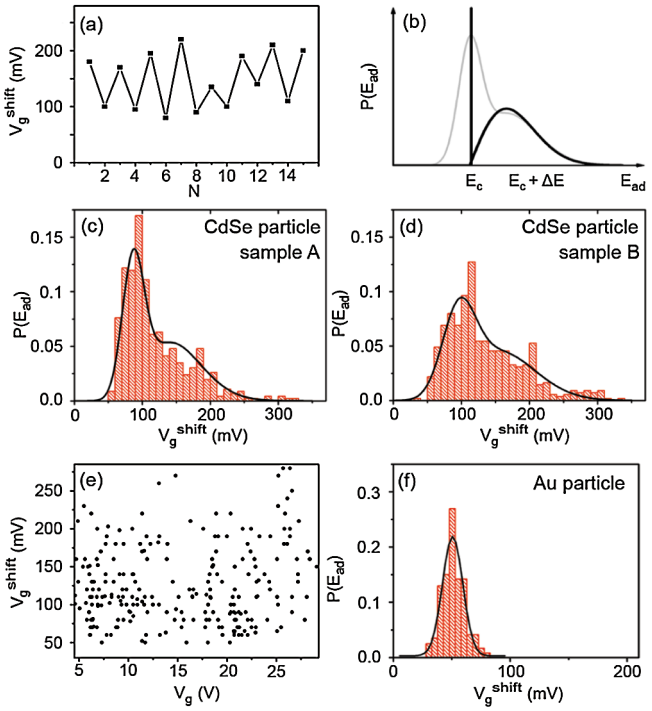

FIG. 4 (color online). (a) Plot of V_g^{shift} for successive N for $V_g \sim 17$ V (sample B). (b) Schematic of bimodal Wigner distribution (black curve). The smearing of the distribution accounts for the experimental noise (grey curve). (c) Spectrum distribution of V_g^{shift}. The solid curve shows the best fit with the bimodal Wigner distribution convolved with Gaussian. The fit gives $\alpha E_c = 86$ mV and $\alpha\langle\Delta E\rangle = 68$ mV. The Gaussian width is 41.2 meV. (d) Spectrum distribution. We obtain $\alpha E_c = 96$ mV and $\alpha\langle\Delta E\rangle = 75$ mV. The Gaussian width is 60 meV. (e) V_g^{shift} as a function of V_g for sample B. (f) Spectrum distribution for a 30 nm diameter gold nanoparticle, measured in the same way as in (c,d). The solid curve represents a Gaussian fit of width 34 meV.

Before comparing the results to the bimodal Wigner distribution, it may be useful to recall the basics of the related model. The energy separation between electron levels (E_{ad}) can be expressed by the sum of the charging energy E_c and the level spacing ΔE. According to the so-called constant interaction model [15–17], it reads $E_{\text{ad}}^N = E_c + \Delta E^N$ when N is even and $E_{\text{ad}}^N = E_c$ when N is odd. This even-odd effect reflects the spin degeneracy of levels, and is consistent with measurements in Fig. 4(a) [18]. The level spacing is very sensitive to the irregularities in the shape of the dots [15–17]. Classically, this leads to chaotic trajectories for the electrons. Quantum mechanically, the level spacing fluctuates randomly as N is increased. The random matrix theory [19] predicts that the addition energy follows the so-called bimodal Wigner distribution when the spin even-odd effect is taken into account:

$$P(s) = \frac{1}{2}\left[\delta(s) + \frac{\pi}{2} s \exp\left(-\frac{\pi}{4} s^2\right)\right], \tag{2}$$

where $s = \frac{E_{\text{ad}} - E_c}{\langle \Delta E \rangle}$ with $\langle\rangle$ denoting ensemble averaging. Figure 4(b) shows the schematic of the distribution. The delta peak corresponds to E_c, which remains constant with N. The smeared peak is associated to ΔE, which is fluctuating with N. This smeared peak is known as the Wigner surmise. Its functional form is simple [second term in Eq. (2)], and it has described experiments in many different research fields on, for instance, large atomic nuclei, hydrogen atoms in strong magnetic fields, or chaotic microwave cavities [16].

The V_g^{shift} distribution is consistent with the bimodal Wigner distribution. The main peak can be assigned to the charging energy, and the tail to the fluctuating level spacing. The distribution can be fitted to Eq. (2) convolved with Gaussian to account for errors in the determination of V_g^{shift}, for instance. Figures 4(c) and 4(d) show a rather good agreement. Using α estimated from [12], we obtain $E_c \approx \langle\Delta E\rangle \approx 20$ mV, consistent with previous transport measurements [3]. (See [12] for a detailed analysis of ΔE.) For purposes of comparison, Fig. 4(f) shows the V_g^{shift} distribution measured on a Au dot. The distribution exhibits a Gaussian profile, which is to be expected, since ΔE is here much lower than E_c.

Most previous measurements on quantum dots have not given evidence for the bimodal Wigner distribution despite

many attempts with, for instance, GaAs, Si, In_2O_{3-x}, or graphene dots [20–26]. To our knowledge, there is one exception [18], but the measurements are carried out on a low number of electronic states and are not discussed in terms of the bimodal Wigner distribution. The absence of bimodal Wigner distribution has generated tremendous theoretical work [20,27–35]. It has been accounted for by either a strong Coulomb repulsion between the electrons in the quantum dot (larger than the Fermi energy) or the deformation of the shape of the dot when sweeping V_g (for quantum dots that are electrostatically defined by gates). In our experiment, the shape of CdSe quantum dots is well defined and should not be affected by V_g. In addition, the Coulomb interaction between two electrons E_{e-e} is lower than the Fermi energy E_F for sufficiently small particles. The interaction parameter r_s given by E_{e-e}/E_F is equal to $d/2a_0N^{1/3}$, d being the diameter and a_0 the effective Bohr radius. Specifically, we have $r_s < 0.27$ for a 5 nm diameter CdSe particle when $N > 10$ ($r_s = 0.6$ for $N = 1$). Thus, the free-particle picture should be valid. We notice that theoretical works [28,30] predict a progressive change from a Gaussian to a bimodal Wigner distribution depending on r_s and the shape deformation strength. More work is needed, especially on device fabrication, to improve the data quality and to see whether the data perfectly match the bimodal Wigner distribution or the data (slightly) deviate from a bimodal Wigner distribution toward a Gaussian.

In summary, we have developed a new technique that allows us to fill or empty a semiconducting quantum dot with many electrons. The ability to shift the Fermi energy by a large amount holds promise for nanoscale or molecular electronics, since the large energy separation between the levels often has limited access to only one level (or a few). Here, we have exploited this finding to study the statistical aspects of the spectrum of the quantum dot. The measured spectrum distribution approaches the bimodal Wigner distribution, which is the most basic prediction of the random matrix theory applied to quantum dots.

We thank J. Moser, D. Cobden, P. Ordejon, N. Lorente, and C. Flytzanis for helpful discussions. The research was supported by an EURYI grant and CARDEQ (FP6-IST-021285-2). M. Z. acknowledges support provided by Marie Curie Grant No. PIEF-GA-2008-220074.

*adrian.bachtold@cin2.es

[1] A. P. Alivisatos, Science **271**, 933 (1996).
[2] D. J. Noris, A. L. Efros, and S. C. Erwin, Science **319**, 1776 (2008).
[3] D. L. Klein *et al.*, Nature (London) **389**, 699 (1997).
[4] U. Banin *et al.*, Nature (London) **400**, 542 (1999).
[5] E. P. A. M. Bakkers *et al.*, Nanotechnology **13**, 258 (2002).
[6] D. J. Norris and M. G. Bawendi, Phys. Rev. B **53**, 16 338 (1996).
[7] M. Shim and P. Guyot-Sionnest, Nature (London) **407**, 981 (2000).
[8] C. Wang, M. Shim, and P. Guyot-Sionnest, Science **291**, 2390 (2001).
[9] D. V. Talapin and C. B. Murray, Science **310**, 86 (2005).
[10] Core-shell CdSe/ZnS quantum dots were employed with an external amine capped long chain hydrocarbon layer. To reduce the tunnel resistance at the dot-nanotube interface, the hydrocarbon layer and the ZnS coating were gently removed in a 3 mM HNO3 solution. The removal of the ZnS was checked using energy dispersive x-ray spectroscopy. Transmission electron microscopy revealed that the crystalline structure of CdSe quantum dots is preserved and that their diameter is ~5 nm.
[11] A. Gruneis *et al.*, Nano Lett. **7**, 3766 (2007).
[12] See EPAPS Document No. E-PRLTAO-102-057925 for supplementary information for (1) electron counting spectroscopy, (2) determination of E_c and $\langle \Delta E \rangle$, (3) spectrum distribution for electrons and holes, (4) electrons tunneling out from the dot. For more information on EPAPS, see http://www.aip.org/pubservs/epaps.html.
[13] M. Yoon *et al.*, Nano Lett. **7**, 2578 (2007) and references therein.
[14] It is possible that our measurement method may not detect the emission of electrons from the dot into the SiO_2, since the emitted electrons roughly remain at the same distance to the tube.
[15] L. P. Kowenhoven *et al.*, *Mesoscopic Electron Transport*, NATO ASI Ser. E (Kluwer, Dordrecht, 1997).
[16] T. Guhr, A. Muller-Groeling, and H. A. Widenmuller, Phys. Rep. **299**, 189 (1998).
[17] D. Ullmo, Rep. Prog. Phys. **71**, 026 001 (2008).
[18] D. H. Cobden and J. Nygard, Phys. Rev. Lett. **89**, 046803 (2002).
[19] M. L. Mehta *et al.*, *Random Matrixes* (Academic Press, London, 1991).
[20] U. Sivan *et al.*, Phys. Rev. Lett. **77**, 1123 (1996).
[21] F. Simmel *et al.*, Europhys. Lett. **38**, 123 (1997).
[22] S. R. Patel *et al.*, Phys. Rev. Lett. **80**, 4522 (1998).
[23] F. Simmel *et al.*, Phys. Rev. B **59**, R10 441 (1999).
[24] S. Lüscher *et al.*, Phys. Rev. Lett. **86**, 2118 (2001).
[25] M. Boehm *et al.*, Phys. Rev. B **71**, 033305 (2005).
[26] L. A. Ponomarenko *et al.*, Science **320**, 356 (2008).
[27] Y. M. Blanter, A. D. Mirlin, and B. A. Muzykantskii, Phys. Rev. Lett. **78**, 2449 (1997).
[28] R. Berkovits *et al.*, Phys. Rev. Lett. **81**, 2128 (1998).
[29] R. Berkovits and B. L. Altshuler, Phys. Rev. B **55**, 5297 (1997).
[30] R. O. Vallejos, C. H. Lewenkopf, and E. R. Mucciolo, Phys. Rev. Lett. **81**, 677 (1998).
[31] G. Hackenbroich, W. D. Heiss, and H. A. Weidenmuller, Phys. Rev. Lett. **79**, 127 (1997).
[32] A. A. Koulakov, F. G. Pikus, and B. I. Shklovskii, Phys. Rev. B **55**, 9223 (1997).
[33] E. Cuevas, E. Louis, and J. A. Verges, Phys. Rev. Lett. **77**, 1970 (1996).
[34] M. Stopa *et al.*, Physica (Amsterdam) **249–251B**, 228 (1998).
[35] P. N. Walker, Y. Gefen, and G. Montambaux, Phys. Rev. Lett. **82**, 5329 (1999).
[36] B. Gao *et al.*, Phys. Rev. B **74**, 085410 (2006).